Geomorphology 281 (2017) 31–42

Contents lists available at ScienceDirect

Geomorphology

journal homepage: www.elsevier.com/locate/geomorph

# The differences in morphological development between the intertidal flats of the Eastern and Western Scheldt

P.L.M. de Vet[a, b, *], B.C. van Prooijen[a], Z.B. Wang[a, b]

[a] Delft University of Technology, Faculty of Civil Engineering and Geosciences, The Netherlands
[b] Deltares, P.O. Box 177, Delft 2600 MH, The Netherlands

ARTICLE INFO

*Article history:*
Received 9 May 2016
Received in revised form 8 December 2016
Accepted 29 December 2016
Available online 3 January 2017

*Keywords:*
Eastern Scheldt
Western Scheldt
Intertidal flats
Human interventions

ABSTRACT

Human interventions have a large impact on estuarine morphology. The intertidal flats in the Eastern Scheldt and Western Scheldt estuaries (The Netherlands) have faced substantial morphological changes over the past decades. These changes are thought to be caused by human interventions, such as the construction of the storm surge barrier in the mouth of the Eastern Scheldt, and the deepening of the navigation channels of the Western Scheldt. This paper analyses several datasets and numerical simulations of hydrodynamics, providing an overview of the various morphological characteristics of the intertidal flats in the two estuaries over time and space. Apart from the volume, area and average height of these areas, also the integral steepness of each flat is quantified based on its full geometry. The analyses focus on the intertidal flats surrounded by water, which allows for a robust comparison between the different flats. The intertidal flats in the Western Scheldt appear to be substantially steeper compared to those in the Eastern Scheldt. The data indicates that a larger average height of a flat is related to a larger steepness. Despite variations in the evolution of the different flats, distinct characteristics of both estuaries are observed. An opposed trend is identified over time: the flats in the Western Scheldt have mainly increased in height, whereas the flats in the Eastern Scheldt have lowered after the completion of the storm surge barrier. This opposing development is associated with differences in tidal flow velocities in the estuaries, which are the result of human interventions.



## 1. Introduction

Morphological changes of intertidal areas threaten the ecological value of estuaries all around the world (Smaal and Nienhuis, 1992; Wilson et al., 2005; Murray et al., 2014). The Eastern Scheldt (ES) and the Western Scheldt (WS) are two neighbouring estuaries located in the southwest of The Netherlands with a substantial amount of intertidal areas (see Fig. 1). Both estuaries face various human interventions, which influence the morphological changes of these systems (Wang et al., 2015). In recent decades, the intertidal flats in the ES were lowering (Louters et al., 1998), whereas those in the WS have mainly been increasing in elevation (Cleveringa, 2013). Further, previous studies suggest that the intertidal flats in the WS have been steepening (e.g., Bolle et al., 2010; Kuijper and Lescinski, 2013), which could induce an impoverishment of the natural habitats (De Jong and De Jonge, 1995; Fujii and Raffaelli, 2008). However, these suggestions are based on individual cross-sections or changes of individual bulk quantities (i.e., height, area or volume of flats), which do not necessarily imply a general steepening of the bed slopes. Knowledge is still limited on how individual intertidal flats are developing within these estuaries and on what causes the differences in morphological development between these flats.

The WS estuary is the Dutch part of the River Scheldt which is connected to the North Sea. From the mouth of the estuary to the Dutch/Belgian border, the tidal range increases from 3.5 m to 5 m. The average river discharge of around 100 $m^3/s$ is very limited compared to the tidal discharges, causing the estuary to be well mixed (Cancino and Neves, 1999; De Vriend et al., 2011). The WS provides access to various harbours, of which the port of Antwerp (Belgium) is the largest. To keep the ports accessible for the cargo vessels of increasing size, the navigation channels were deepened to 14.5 m in the 1970s and deepened further to 16 m around 1997 (De Vriend et al., 2011). More recently, the channels where deepened by another 1.2 m in 2010. Most of the yearly dredged sediment is dumped at assigned areas within the estuary. Large parts of the intertidal areas had already been reclaimed before these dredging activities took place (Van den Berg et al., 1996). The intertidal areas surrounded by

* Corresponding author at: Stevinweg 1, room S3.00.90, 2628 CN, Delft,The Netherlands.
*E-mail address:* p.l.m.devet@tudelft.nl (P. de Vet).

http://dx.doi.org/10.1016/j.geomorph.2016.12.031
0169-555X/

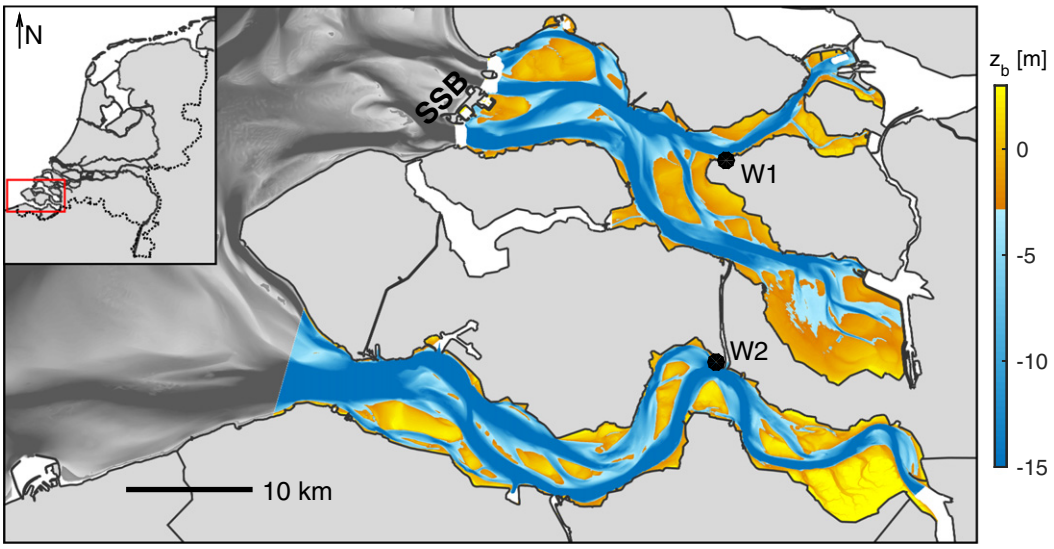


**Fig. 1.** Overview of the Eastern Scheldt (North) and Western Scheldt (South). The Eastern Scheldt is partially closed by the storm surge barrier (SSB). Areas with no bathymetric data are marked white. The bathymetric data (source: Rijkswaterstaat) is with respect to NAP (Dutch Ordnance Level). The dots indicate the wind measurement stations Stavenisse (W1) and Hansweert (W2).

water in the WS are characterized by a typical grain size of 50–150 μm ($D_{50}$), and contain typically less than 10% mud (Van Eck, 1999). However, there are regions with higher mud fractions on several flats.

In contrast, the ES has no river inflow as it is only in connection to the North Sea. In the past, the ES was also linked to neighbouring estuaries including the WS. During the past centuries, land reclamation projects have been taken place in the ES (Eelkema et al., 2009). After the North Sea flood of 1953, the Dutch government initiated the Delta Project to protect the southwest of The Netherlands against flooding. In 1986, the storm surge barrier (SSB in Fig. 1) was completed, closing the estuary under severe storm conditions and constricting the discharge during regular conditions. In the same project, various other dams were constructed, closing off the remaining openings of the estuary. All these interventions induced substantial changes to the tidal flow velocities and reduced the tidal range by more than half a meter, which currently ranges between 2.5 m and 3.5 m (Louters et al., 1998; Eelkema et al., 2009). The intertidal areas near the mouth of the ES are characterized by a typical median grain size of around 200 μm ($D_{50}$), whereas further from the mouth grain sizes in the order of 150 μm are more typical (Kohsiek et al., 1987).

The impact of the interventions in the ES and WS on the morphological processes of the intertidal areas in these systems can be related to changes in the physical processes. Eisma (1998) and Le Hir et al. (2000) indicate that the tide, the waves, the wind-induced circulation, the density-driven circulation and the drainage are important processes for sediment transport on intertidal areas. Friedrichs (2011) presents a qualitative understanding, supported by idealised numerical models and field observations, of the shape and morphological response of intertidal areas related to changes in the forcing. Friedrichs indicates that a variation in the relative importance of the tide to the waves induces changes in the geometry of these flats. This framework is in line with the findings of Louters et al. (1998) and Wang et al. (2015), who argued that the reduction of the tidal flow in the ES caused a relative increase of the erosive effects of waves. According to Green and Coco (2014), there is sufficient evidence to conclude that waves erode and tidal currents cause accretion of intertidal areas on the long term.

Previous studies applied various methods to analyse datasets of intertidal areas. For example, Dyer et al. (2000) applied a cluster analysis to produce a classification scheme of mudflat types, considering several mudflats in European estuaries with various hydrodynamic, geometric, biological and sediment characterising variables. Bearman et al. (2010) focussed on the shape of intertidal areas, by analysing eigenfunctions of cross-shore profiles in San Francisco Bay. With this approach, a correlation was revealed between the degree of convexity or concavity of profiles and the rate of deposition, tidal range, fetch length, grain size and tidal flat width. Santinelli and de Ronde (2012) analysed cross-sections measured on the intertidal areas in the ES, identifying an average erosion trend of 0.9 cm per year. In addition, other studies applied a more descriptive approach to identify local morphological characteristics of individual intertidal areas in more detail (e.g., Cleveringa, 2013).

This study focusses on identifying and understanding the state and temporal development of the morphology of individual intertidal flats in the ES and WS. The analyses are limited to the major intertidal areas which are surrounded by water at MLW (see Fig. 2), as it is not straightforward to robustly define the boundaries of intertidal flats adjacent to the land. Still the methodology of this study could be applied to those intertidal flats with a land boundary, but the lateral boundaries require case-dependent definitions which make these areas less applicable for comparison studies. Appropriate bulk properties are derived from full-domain digital elevation models. For each intertidal flat, the area, volume and average height are determined. Changes in these parameters are relevant indicators for the ecological development of intertidal flats, as a clear relation exists between the vertical distribution of species and the immersion period of a flat (Wolff, 1973). Further, the methodology of Strahler (1952) is applied to robustly describe the steepness of intertidal flats, without the use of arbitrary cross-sections. By analysing the hydrodynamic forcing, a possible explanation for identified morphological differences between flats is given.

## 2. Field and model data

### 2.1. Datasets

In recent decades, data on the morphology of tidal flats have been gathered in both estuaries. Various digital elevation models provide a spatial coverage of the bathymetry of the intertidal areas. The

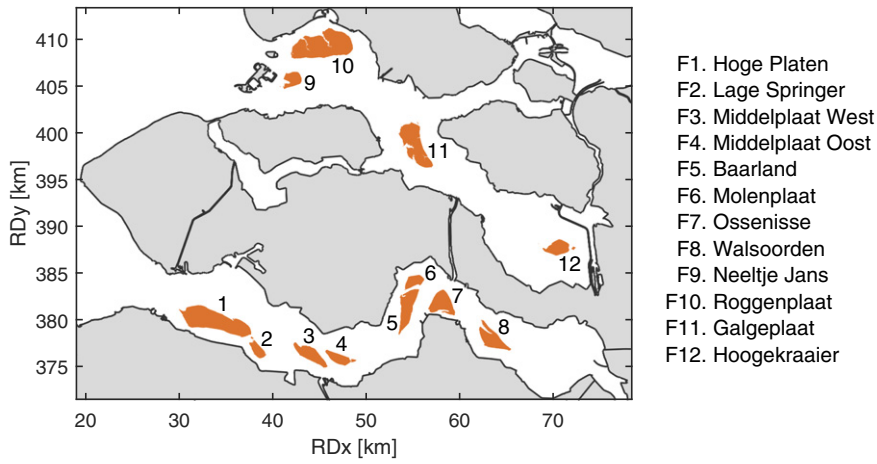


**Fig. 2.** The studied intertidal areas in the WS (flats F1–F8) and in the ES (flats F9–F12). The individual tidal flats are sorted with increasing distance from the mouth.

so-called *Vaklodingen* dataset covers both estuaries with a grid resolution of 20 m (Marijs and Paree, 2004; Wiegmann et al., 2005). This dataset combines single beam measurements at 100/200 m transects with GPS Real-Time Kinematic (RTK) measurements on top of the tidal flats (with more primitive levelling techniques before GPS-RTK existed). Since 2001, the dry parts of the estuaries have also been measured with the Light Detection and Ranging (LiDAR) technique. This dataset is included in the Vaklodingen dataset, but it is also available separately on a finer grid with a resolution of 2 m or 5 m. Parts of the data with documented measurement mistakes (Marijs and Paree, 2004) are excluded from this research. In this study, the high resolution LiDAR data are preferred. The Vaklodingen dataset is analysed for the long-term analyses, which also includes measurements before 2001.

Wiegmann et al. (2005) estimated the vertical accuracy of the Vaklodingen dataset at 50 cm ($2\sigma$), independent of whether the data is measured by single beam or with RTK, as the interpolation process dominates this error. The LiDAR data is considered as slightly more accurate, approximately 30 cm ($2\sigma$). However, as this study considers cumulative quantities, the net inaccuracies reduce substantially. For a large number of grid cells, the cumulative interpolation error averages out. Systematic errors could still be present if a large amount of cells are considered, these are especially substantial in the old data by less accurate measurement techniques and could be in the order of 10 cm (Marijs and Paree, 2004).

Additionally, various cross-sections have been measured by Rijkswaterstaat (part of the Dutch Ministry of Infrastructure and the Environment) in great detail for over 25 years. These cross-sections are especially useful for analysing local morphological changes. In this study, some of the cross-sections are presented to indicate the diversity in geometry and morphological response of the system and to analyse morphological changes at shorter time scales than the temporal resolution of the Vaklodingen dataset. According to Wiegmann et al. (2005), the accuracy of those measurements can be estimated at 6 cm ($2\sigma$).

Rijkswaterstaat provides long-term measurements of the water levels, waves and wind at various stations in the ES and WS. By the presence of the storm surge barrier in the ES, the majority of the waves is generated inside this estuary (Louters et al., 1998). The mouth of the WS is exposed to waves from the North Sea, but further inside the estuary, the waves are expected to be mainly generated locally. The wave climate at individual locations is not considered as it depends highly on local geometry. Instead, the wind climate, driving the wave generation within the estuaries, is presented for two centrally located measuring stations in Fig. 3.

### 2.2. Numerical model results

Existing numerical model schematizations with Delft3D (Lesser et al., 2004) provide spatial distribution information on the hydrodynamics. The ScalOost model describes the full ES and ranges up to 30 km offshore, taking the damping effect of the storm surge barrier into account (Pezij, 2015). In the WS, the NeVla model is shown to provide reliable predictions of the hydrodynamics (Van der Werf et al., 2015).

The spatial distribution of the tidal range (MHW-MLW) can be estimated based on the modelled hydrodynamics (see Fig. 4a). The modelled tidal range deviates not more than 0.10 m from the water level measurements for the full year of 2014. A robust estimate for the tidal range for each individual tidal flat can therefore be derived. Another relevant hydrodynamic indicator is the average magnitude of the flow velocities in the estuaries (see Fig. 4b). Clearly, the tidal range is not a proper indicator for the local flow velocities, as the tidal flow velocities might be very small in channels with a relatively large tidal range (e.g., around Hoogekraaier (F12)). Therefore, both indicators should be considered individually, if the hydrodynamic forcing on intertidal flats is concerned.

## 3. Methodology

Hypsometric curves provide valuable insights into morphodynamic systems (Boon and Byrne, 1981; Strahler, 1952). In various previous studies, hypsometric curves are considered for whole basins or sections of these (e.g., Dieckmann et al., 1987; Kirby, 2000; Stanev et al., 2003; Wang et al., 2002; Kuijper and Lescinski, 2013). However,

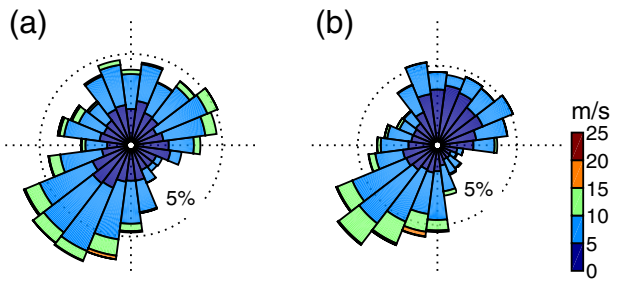


**Fig. 3.** Wind climate of 2013 at (a) Stavenisse (ES) and (b) Hansweert (WS), based on measurements by Rijkswaterstaat (HMCZ). The locations of the measurement stations are indicated in Fig. 1.

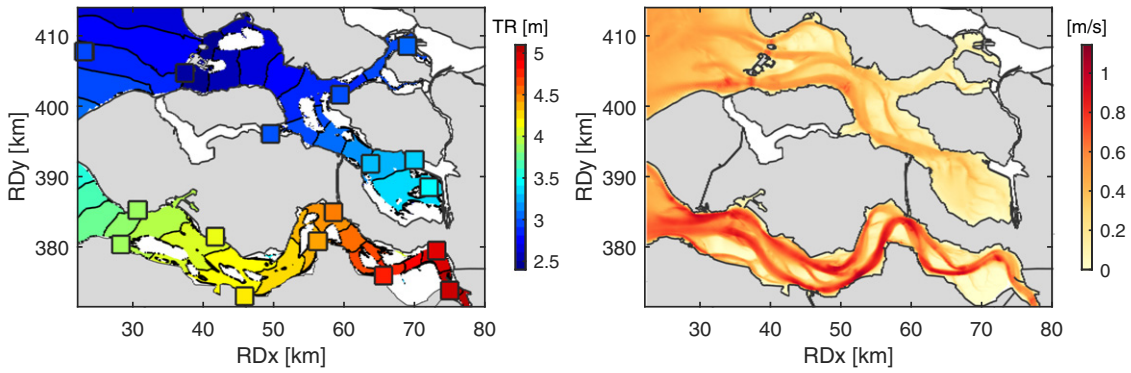


**Fig. 4.** A spatial overview of (a) the tidal range and (b) the average magnitude of the depth-average flow velocities, computed with a one-month model run (August 2014) of the ScalOost model (ES) and the NeVla model (WS). The black contour lines in (a) illustrate 0.1m intervals of the tidal range and the coloured squares present the tidal range calculated from the full 2014 time series of the water level stations of Rijkswaterstaat. (For interpretation of the references to colour in this figure legend, the reader is referred to the web version of this article.)

this study focusses on the characteristics of individual flats. Therefore, the hypsometric curves of individual flats are studied, which are constructed by the following procedure (illustrated in Fig. 5):

(a) Polygons are drawn around the MLW line of the targeted tidal flats. The polygons are not necessarily the same for all considered years, because tidal flat planform changes as the morphology evolves;
(b) The grid cells within the polygon and of which the bed level is between MLW and MHW, are considered as the intertidal region of the flat, all other grid cells are discarded;
(c) The hypsometric function $A(z) = A(Z > z) - A(Z > \text{MHW})$ is obtained by multiplying the surface area per grid cell with the number of grid cells of which the bed level is larger than $z$, but smaller than MHW.

Because of the large spatial inhomogeneity of the tidal range (see Fig. 4a), a local estimate for the tidal range is made for each tidal flat, instead of a single one for each estuary. Regions with vegetation are considered part of the tidal flats as long as these are between MLW and MHW.

In addition to the hypsometric curve, the volume distribution of a flat $V(z) = V(Z > z) - V(Z > \text{MHW})$ can be derived by including the bed level per grid cell in step (c). Based on these functions, the average height of an intertidal area with respect to MLW follows as:

$$h = \frac{V(Z > \text{MLW}) - V(Z > \text{MHW})}{A(Z > \text{MLW}) - A(Z > \text{MHW})}. \quad (1)$$

The determination of the bed slope of a tidal flat is arbitrary, if based on cross-sections. First, a cross-section is not necessarily perpendicular to all depth contours. Second, a limited amount of cross-sections are not necessarily representative of the full inhomogeneous geometry of a flat. In this study, the integral method of Strahler (1952) is considered (originally developed for drainage basins), such that the full morphology of the flats is accounted for.

Strahler (1952) showed that the bed slopes of a digital elevation model are related to the derivative of the hypsometric curve and the length of the contour lines. Consider the decrease of the surface area $\Delta A$ between the contour lines, when the elevation level increases from $z - \Delta z/2$ to $z + \Delta z/2$ (see Fig. 6). In this study, a small value of 1 cm is used for $\Delta z$. This surface area decrease divided over $P(z)$, the length of the contour lines at $z$, results into the average horizontal shift of the contour line ($\Delta\bar{s}$):

$$\Delta\bar{s} = -\frac{\Delta A}{P(z)}. \quad (2)$$

With this average horizontal shift of the contour line, the integral bed slope at a certain bed level elevation can be evaluated as follows:

$$\frac{dz}{d\bar{s}} = \lim_{\Delta\bar{s}\to 0}\frac{\Delta z}{\Delta\bar{s}} = \lim_{\Delta A\to 0} -P(z)\frac{\Delta z}{\Delta A} = \lim_{\Delta A\to 0} -P(z)\frac{1}{\frac{\Delta A}{\Delta z}} = -P(z)\frac{1}{\frac{dA}{dz}}. \quad (3)$$

The derivative $\frac{dA}{dz}$ in this formulation is readily evaluated from the hypsometric function $A(z)$. The hypsometric function is slightly smoothed, with a moving average over a depth of 20 cm, to get to a proper derivative without local non-physical numerical steps. These

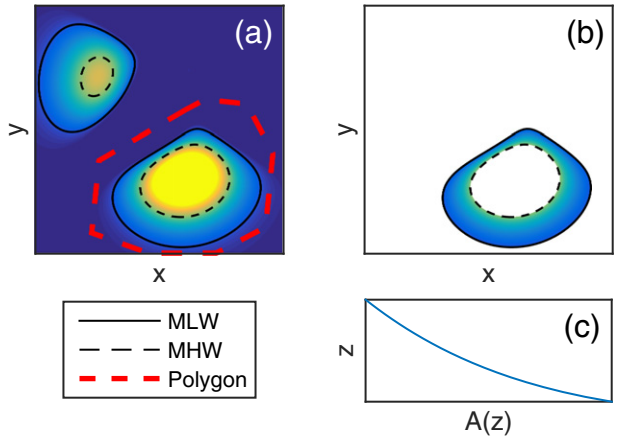


**Fig. 5.** The three steps to derive the hypsometric curve of an individual tidal flat (example with synthetic data).

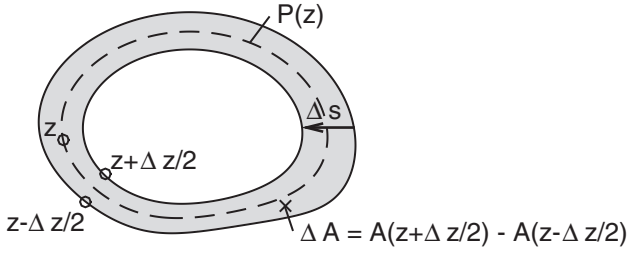


**Fig. 6.** Illustration derivation bed slopes.

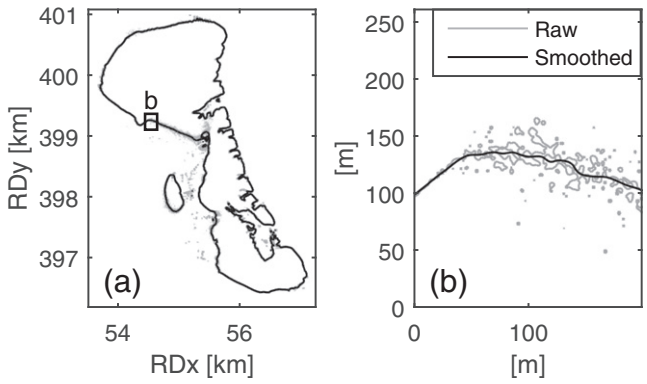


**Fig. 7.** The MLW+0.5m contour lines for the Galgeplaat (F11). Both the contour lines as calculated with the raw bathymetry data and as calculated with the smoothed data are presented.

are present as discrete bathymetric data is considered. The determination of the perimeter $P(z)$ is sensitive to the resolution of the bathymetric data and to noise in these data. Therefore, the digital elevation models are interpolated to the same 2 m × 2 m grid and smoothed with a Gaussian convolution filter ($\sigma = 5$ cells $= 10$ m, resulting average RMSD of 0.06 m). The derived perimeter represents the main geometry, instead of the noise (see Fig. 7). This essential smoothing process affects the magnitude of the perimeter, and with that also the magnitude of the calculated bed slopes. Nevertheless, a comparison between the bed slopes of different tidal flats is robust, as precisely the same settings are used for all flats in all studied years. As the top of the flats are described by a small amount of data points, the upper 5% of the intertidal area are excluded from the analysis. Otherwise, inaccuracies in the small amount of data points dominate these results.

## 4. Results

### 4.1. Present morphological state of the intertidal flats

To compare the intertidal areas between both systems, aggregated morphological changes of the intertidal flats during recent years are presented in Fig. 8. This figure shows the average height, total area and total volume of all studied flats for each estuary. The total area of the studied flats in the ES is 25% smaller compared to those in the WS. However, the larger tidal range in the WS causes the intertidal volume of the ES flats to be 75% smaller than the intertidal volume of the WS flats. This difference in intertidal volume is also due to the substantially lower flats in the ES. Fig. 8 indicates the flats in the ES to be on average more than 0.75 m lower compared to the WS flats, with respect to NAP (Dutch Ordnance Level).

Fig. 8 also shows the recent changes over time of the intertidal tidal flats in both estuaries. Although the tidal flats in the WS have mainly increased in elevation, the intertidal volume of these flats has remained more or less constant as the intertidal area was reduced at the same time (i.e., a general steepening of the hypsometry of the intertidal flats). Over these years, the ES has faced substantial intertidal sand losses, indicated also by the decrease of the average height and area of its intertidal flats. Although previous studies did not define the tidal flats with respect to the local tidal range, the lowering of the flats in the ES, and the heightening of the flats in the WS, are in line with the findings of Louters et al. (1998) and Cleveringa (2013). The data indicates that the heightening of the flats in the WS appeared to be fairly linear, whereas the full change in the bulk parameters for the ES appeared during the first half of the considered period. Nevertheless, it is hardly possible to draw conclusions on the morphological evolution with such a limited amount of data points.

The geometry and evolution of the individual intertidal flats are of interest, to reveal the similarities and differences between the flats. For this purpose, Fig. 9 presents the hypsometric curves for each flat studied. These curves indicate the total area of each intertidal flat and how this area is distributed over the elevation of these flats. A large diversity in the geometry is evident. Some of the hypsometric curves appear to be fully concave-up, some are fully convex-up and others are a combination of both. However, the shape of these curves does not provide direct insight into the shape of the bed profiles, as the shape of the hypsometric curves should be corrected for the perimeter variation over depth first (Eq. (3)). Apart from Ossenisse (F7) and Walsoorden (F8), the height of the flats with respect to NAP reduces with the distance from the mouth of the estuaries.

Apart from the relatively small Lage Springer (F2), all the flats in the WS have been rising over these years. This is in contrast to the trend in the ES, where the flats have been lowering consistently. The almost uniform decrease of the hypsometric curves in the ES indicates that the flats in the ES have been lowering over the full vertical range of the flats. In the WS, a comparable uniform, but opposing, vertical shift of the hypsometric curve was present for Hoge Platen (F1) and Middelplaat Oost (F4). For other flats in the WS, a reduction

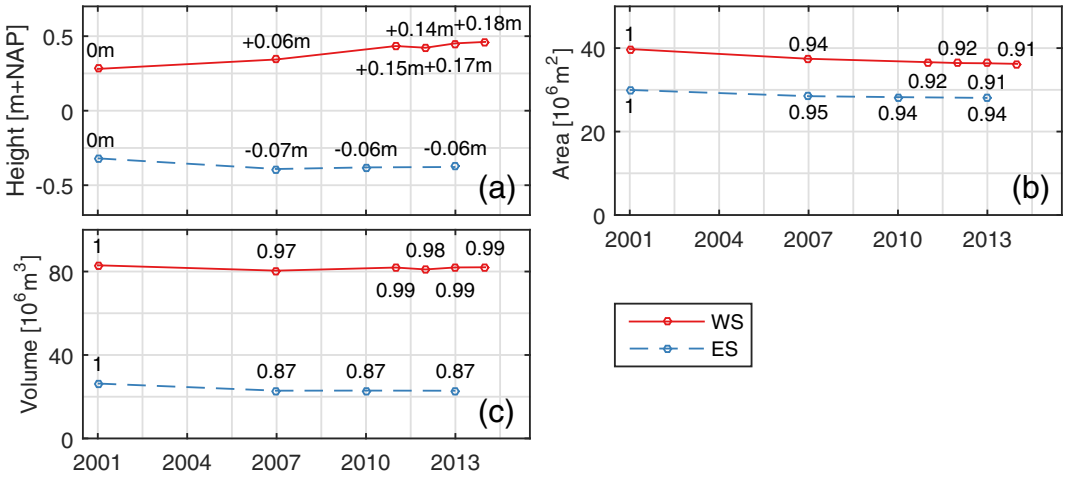


**Fig. 8.** Recent changes of (a) the intertidal height, (b) the area and (c) the volume of the studied tidal flats in each estuary, based on the LiDAR data. The aggregated intertidal height is a weighted average, with respect to the area of each flat. The numbers in (a) indicate the absolute changes whereas the numbers in (b) and (c) show the changes relative to the initial (2001) values.

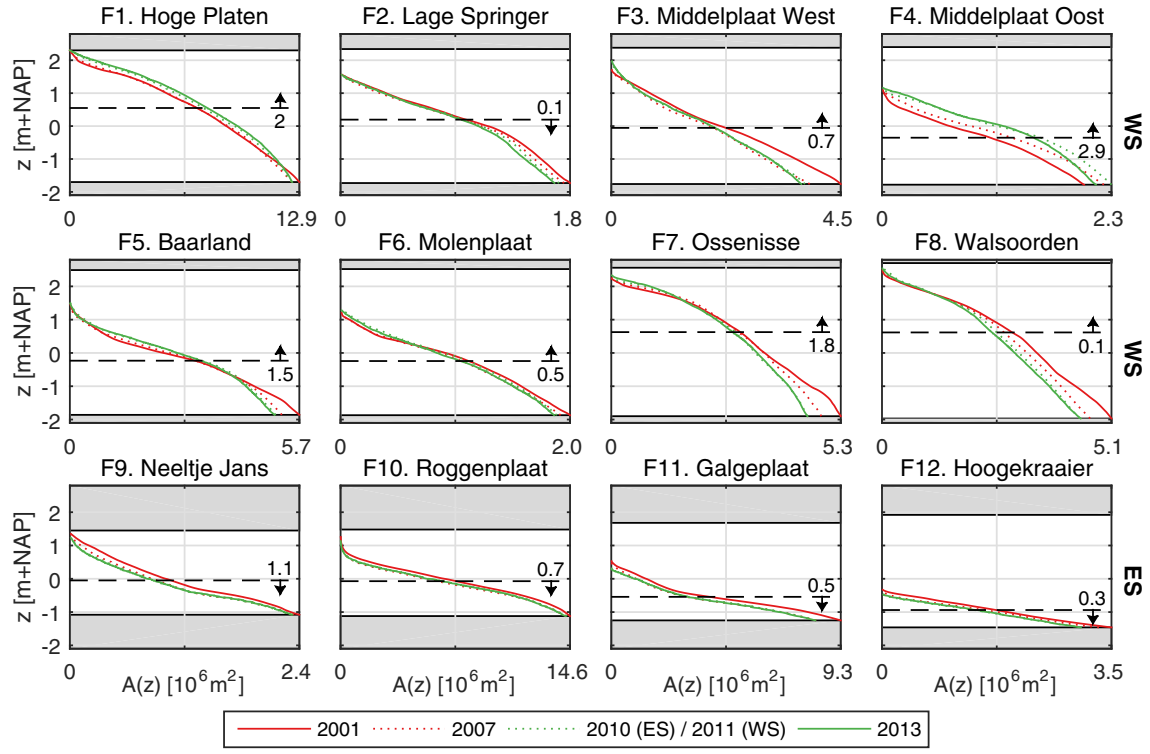


**Fig. 9.** Comparison of the hypsometric curves between MLW and MHW for the eight tidal flats in the WS and the four flats in the ES (ordered with increasing distance from the mouth) based on the LiDAR data. The gray areas indicate the elevations outside of the mean tidal range. The horizontal dashed lines illustrate the average height of each intertidal flat in 2001. The arrow indicates whether the average height increased or decreased from 2001 to 2013, the number next this arrow expresses the average change in average height of the flat per year in centimetres. The 2012 and 2014 data of the WS are not considered in this figure, to enhance readability.

of the area at MLW in combination with a heightening of the higher parts of the flats, indicates a steepening of the hypsometric curves. The evolution of Lage Springer (F2) and Walsoorden (F8) illustrates that an almost constant average height does not necessarily imply a flat to be in equilibrium, as the decrease in area was still substantial for both flats. This illustrates the importance to analyse the various bulk properties simultaneously.

Although the shape of the hypsometric curves provides insight in the geometry of the flats, these curves should be combined with their perimeters to result in an actual representation of the bed slopes, as discussed in Section 3. The integral bed slopes for the 2013 LiDAR data are provided in Fig. 10 over the full tidal range, for each estuary. Generally, milder bed slopes are found at higher elevations. Apart from some fluctuations at the lower elevations, the integral bed slopes appear to be approximately linearly decreasing with the bed level elevation (i.e., bed profiles are on average convex-up). A clear distinction is visible between the flats in the ES and those in the WS: the flats in the ES are substantially flatter compared to the WS flats. The difference in steepness between the flats in the two estuaries is more than 50% around NAP+0 m (roughly MWL). At the same time, there are differences between the intertidal areas of each estuary. The flattest of all these intertidal areas is Hoogekraaier (F12), which is also the lowest one (Fig. 9). Consistently, the steepest of the flats, Ossenisse (F7) and Walsoorden (F8), are also the highest ones.

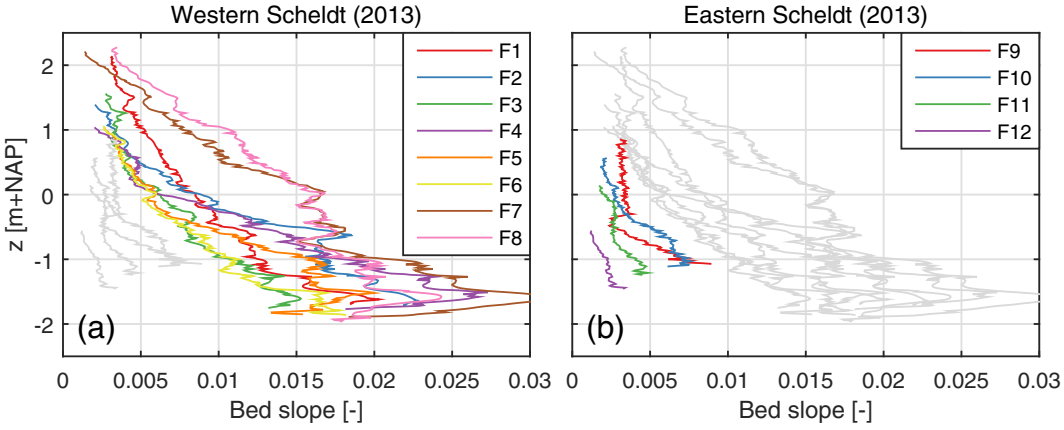


**Fig. 10.** The integral bed slopes for (a) the WS and (b) the ES, based on the 2013 LiDAR dataset. In each figure, the flats of the other estuary are plotted in light gray. Details of the derivation are provided in Section 3.

These two steepest flats were the only flats opposing the relation between the height of the flats and the distances from the mouth of each estuary.

### 4.2. Long-term morphological changes

As the LiDAR data have been measured only since 2001, the lower resolution Vaklodingen dataset is studied to assess the long-term tendency of the flats. The tidal range is considered constant over time in the long-term analyses, by using the spatial distribution of Fig. 4a. With this approach, the focus of this study is on the pure morphological changes, and not on the influence of changes in tidal range on the bulk parameters. Fig. 11 provides the evolution of the average height, area and volume for the WS flats over a measurement period of 59 years (1955–2013), and for the ES flats over a measurement period of 45 years (1968–2013). As Walsoorden (F8) was merged with the mainland in the past, this flat is considered only after 1989. The substantial changes of the bulk parameters of the WS flats, measured on average once every 1.8 years, indicate that the long-term changes exceed the inaccuracies of the data (which is in the order of 10 cm, see Section 2.1). In contrast, the ES data should be analysed with more restraint as the maximum changes in bulk parameters are closer to the order of magnitude of the measurement errors. As well as these were measured on a substantially larger average interval of 5.5 years, providing a maximum of eight points over time per flat.

These long-term data indicate that the flats in the WS, especially the large Hoge Platen (F1) and Ossenisse (F7), have increased in height fairly monotonically after 2001 (also in accordance with Fig. 8). However, this continuous tendency does not hold for all other flats in the estuary. For example, Molenplaat (F6) and Walsoorden (F8) lowered over four succeeding years after the third deepening project (2010). If the full measurement period is considered, the average height, area and volume fluctuated over time for almost all flats. For Ossenisse (F7), one of the most dynamic flats, these bulk quantities faced a substantial net increase over time, despite the fluctuations. Over this period, the intertidal volume of this flat has increased up to 430% of its original value. In contrast, the area and volume of Middelplaat Oost (F4) fluctuated around an almost constant value. Fig. 11 indicates that these fluctuations could be related to the deepening projects of the WS, as these coincide with some of the major changes in the trends, especially around the second deepening project. Nevertheless, this is not the case for all the flats and there were also other activities ongoing over these 59 years (e.g., dredging and dumping projects). Especially around the flats with sudden changes in area and volume (Middelplaat Oost (F4) and Ossenisse (F7)) there were frequently dredging and dumping activities. Despite the non-uniform long-term evolution of the WS flats, the aggregated average intertidal height, weighted with respect to the area of each flat, increased from NAP−0.12 m around 1955 to NAP+0.45 m in 2014. This implies an average increase in height of almost 1 cm per year. The mean absolute deviation of the average heightening rate between the flats equals to 0.5 cm per year.

A clear change in the trend of the evolution of the ES flats are indicated by the results. Before the completion of the storm surge barrier, all flats for which data is available increased in height. Although this is supported by just two measurement points for each flat, the observed changes are substantial: an heightening up to 0.3 m for Neeltje Jans (F9). After the barrier was completed, all flats in the ES faced net erosion. For Galgeplaat (F11) and Hoogekraaier (F12), the bulk parameters changed quite continuously, whereas this is not the case for Neeltje Jans (F9) and Roggenplaat (F10). The latter could be caused by inaccuracies of the historical data, as the morphological changes are in the order of the measurement error. If all ES flats are aggregated, the data indicates a net lowering from NAP−0.17 m in 1983 to NAP−0.38 in 2013, which equals to an average lowering rate of 0.7 cm per year. This lowering coincided with a net decrease in the volume of the flats (25–50%) which was substantially larger than the net decrease of area of the flats (9–27%). As also indicated

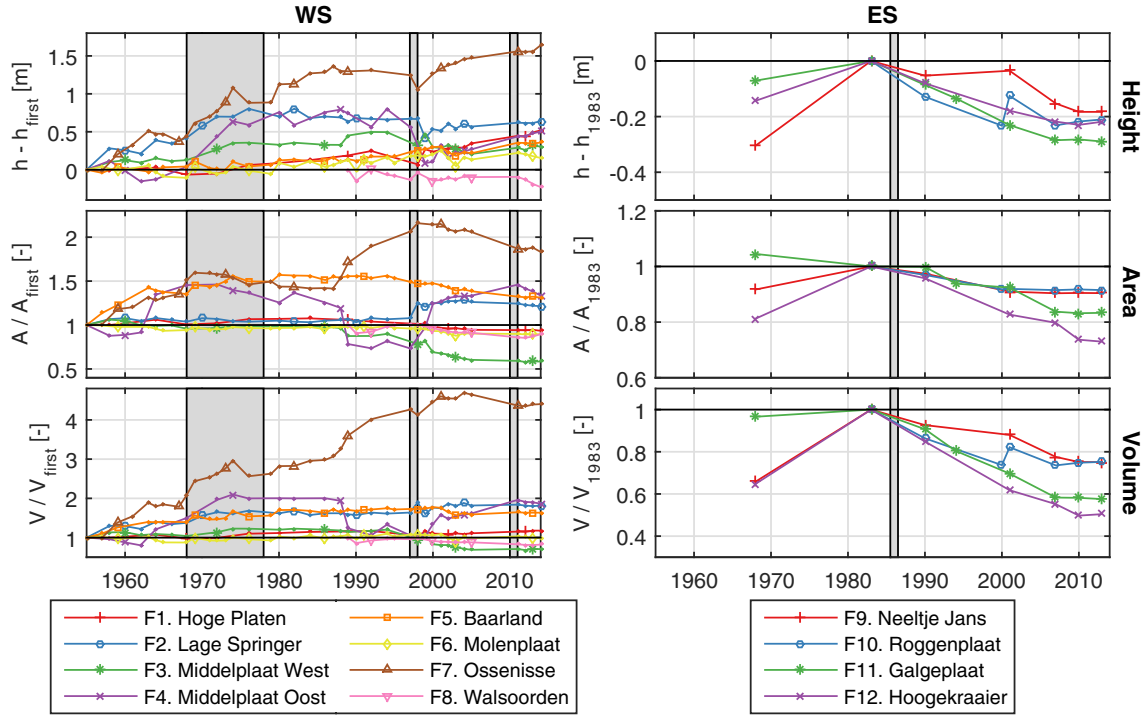


**Fig. 11.** Long-term changes of the average height, area and volume of all studied flats of each estuary as derived from the Vaklodingen dataset. For the WS, the data are presented relative to the first measurement year: 1989 for Walsoorden (F8) and around 1955 for all other flats. The data in the ES is presented relative to the last measurement year before the completion of the storm surge barrier (1983). The vertical gray boxes on the background indicate the deepening projects in the WS and the completion of the storm surge barrier of the ES.

by Fig. 8, the changes in the bulk parameters over the recent years (2007–2013) was small compared to the changes in the past.

Three of the studied flats contain a substantial amount of frequently measured cross-sections: Neeltje Jans (F9), Roggenplaat (F10) and Galgeplaat (F11). By the relatively limited amount of Vaklodingen data in the Eastern Scheldt, 7–8 measured years per flat, these are a valuable addition for insights on the temporal changes. The evolution of the average height of the cross-sections of each flat are presented in Fig. 12. The mismatch in the average height between the Vaklodingen data and the average height of the cross-sections is because the elevation of the cross-sections is not necessarily representative of the full intertidal area. For example, the Neeltje Jans (F9) cross-sections are located on the low parts of the flat. Nevertheless, the cross-sectional data indicates that the period of negligible changes of the average height between 2007 and 2013, as observed with the Vaklodingen dataset (Fig. 11), was probably not a measurement artefact. Especially for a large proportion of the cross-sections at the Roggenplaat (F10) (profiles 3–6), a change in trend is visible around 2007. Before 2007, an almost linear lowering of the average height appeared for these profiles, whereas their average height was fairly constant afterwards. The constant average heights of the profiles do not imply that the Roggenplaat (F10) did not erode locally, e.g., horizontally propagating bed forms were still present. However, they do indicate that the net differences between erosion and accretion reduced over time.

The evolution of the bulk parameters (i.e., average height, volume and area) of the flats do not provide direct insight on the evolution of their hypsometry. To this extent, Fig. 13 presents the evolution of the area of each height class over time (i.e., discretized hypsometric curves). In line with the observations related to Fig. 9, a diverse behaviour of the flats is present. Hoogekraaier (F12) is a good example of a flat of which the hypsometry lowered almost uniformly after the completion of the storm surge barrier. In contrast, Molenplaat (F6) faced a slight reduction of the total intertidal area since 1955, whereas the highest heightclasses showed a contrary increase in area. Based on this figure, the sudden changes of Middelplaat Oost (F4) could better be understood. The reduction of the intertidal area just before 1990 did not change the average height of the flat as all height classes faced a more or less similar decrease, whereas the average height decreased just before 2000 by an increase of the low elevations and a decrease of the high elevations of the flat. The latter is evidence for the non-uniformity of the morphological changes of an individual flat at different elevations.

The long-term evolution of the integral bed slopes is presented in Fig. 14. Clearly, the steepness of the flats did not evolve monotonous over time. Within a decade, the integral bed slope could halve or double. Especially for the morphologically active Middelplaat Oost (F4) and Ossenisse (F7), the vertical profiles of the integral bed slopes have been highly variable over time. Certainly, those two flats steepened over the past decade. The other intertidal flats in the WS did not show such a strong increase in steepness over this period, or even a slight flattening (e.g., Molenplaat (F6)). The bed slopes did not change necessarily uniformly over depth. For example, the lower part of Ossenisse (F7) steepened over the past decade, whereas the higher regions of the flat remained more or less unchanged. Based on the vertical diversity in the changes of the bed slopes and on the fluctuations in the bed slopes over the past 59 years, the intertidal flats in the WS could not be classified as purely steepening flats. After the construction of the storm surge barrier, especially the lower regions of the ES flats flattened slightly. Nevertheless, the flats in ES were already substantially milder than those in the WS before the construction of the storm surge barrier.

The vertical shift of a certain integral bed slope corresponded, at least roughly, with the change of the average height of these flats. This indicates that the time scales of these indicators are related to each other. Further, Fig. 10 suggests that also the absolute value of the steepness might be related to the absolute value of the height of a flat, as the steepest flats corresponded to the highest ones, and vice versa. To test this relation, Fig. 15 compares the height of the intertidal areas above MLW with the bed slopes at MWL. These variables are found to be significantly correlated. This relation is not necessarily linear, as a better fit could be achieved by allowing more degrees of freedom. Further, this relation holds for a great variety of reference levels. However, at the high and low elevations, this relation is not significant, which might be explained by a small amount of intertidal flats covering these elevation levels.

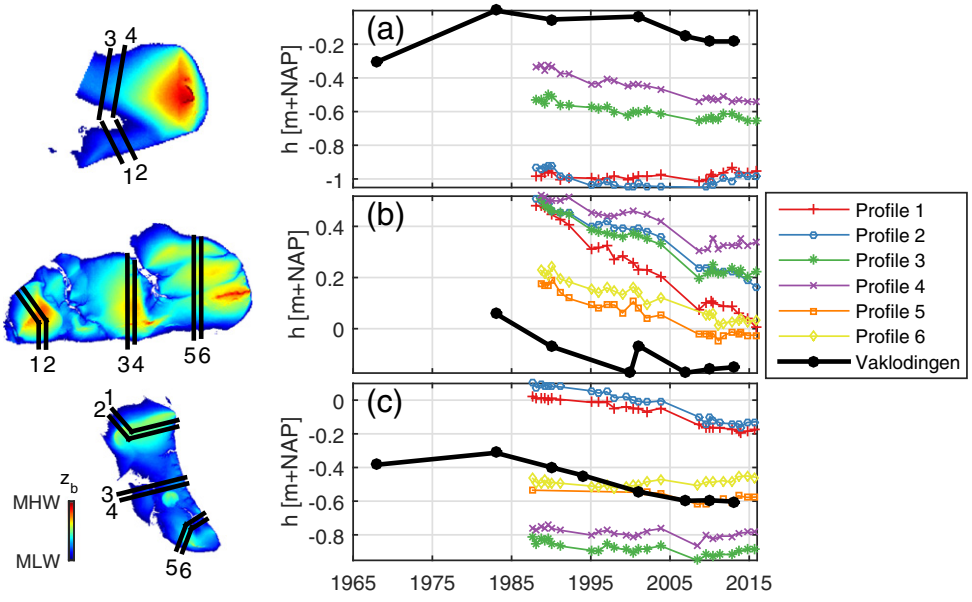


**Fig. 12.** Comparison of the height evolution between the Vaklodingen dataset and the cross-section data for (a) Neeltje Jans (F9), (b) Roggenplaat (F10) and (c) Galgeplaat (F11). Measurement campaigns that covered only a small part of the cross-sections are not considered, and only the parts of cross-sections that were measured in all considered years are taken into account. The positions of the cross-section profiles are indicated on the accompanying maps, which are not on scale (see Fig. 2).

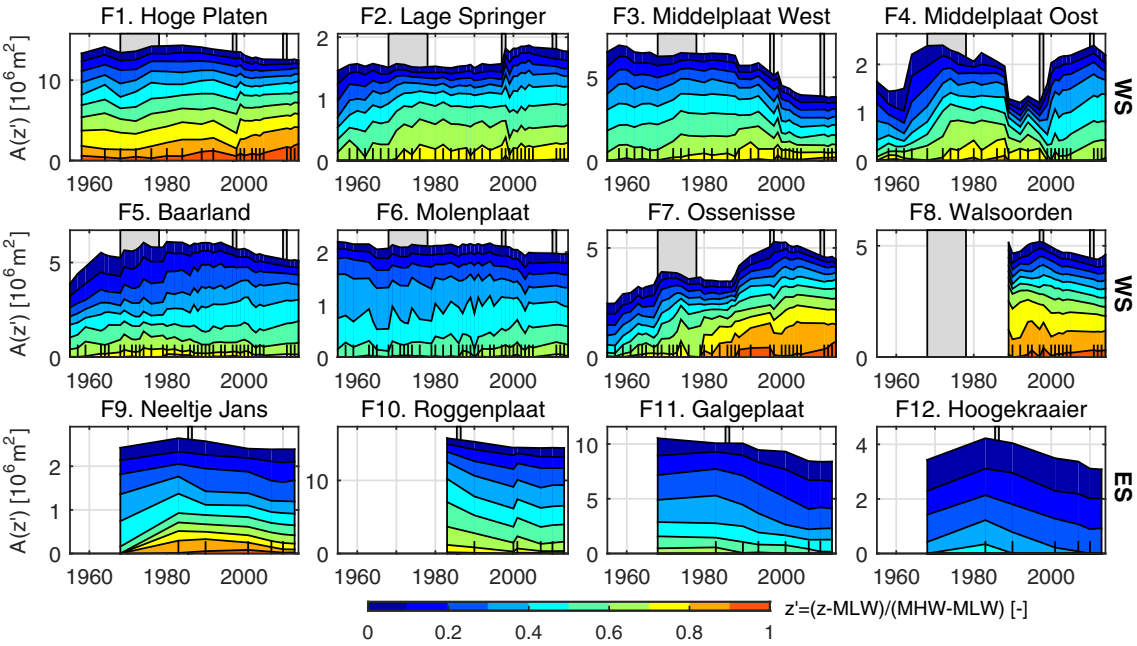


**Fig. 13.** Evolution of each height class per flat over time as calculated with the Vaklodingen dataset. The height classes are relative to the tidal range (MHW: $z' = 1$, MLW: $z' = 0$). The vertical gray boxes on the background indicate the deepening projects in the WS and the completion of the storm surge barrier of the ES.

## 5. Discussion

### 5.1. Limitations of the indicators for the morphology

Various indicators can be used to express the geometrical state of an intertidal flat: the volume, area, average height and integral steepness of these areas. The local variability is lost with these indicators, as they aggregate the full geometry of an intertidal flat. However, the profile of the flats can be substantially different at zones exposed to waves compared to sheltered ones (Friedrichs, 2011). For example, Fig. 16 indicates some of the spatial inhomogeneity around Galgeplaat (F11). At the northern cross-section (a), a locally concave-up profile has been formed, being evidence for an increased importance of waves (in line with Friedrichs, 2011). Such a concave-up profile formation was not visible at the southern cross-section (c), where the wind fetch is much shorter. Still, valuable insights have been achieved into the general morphological trends of the intertidal flats in the ES and WS, by analysing trends in these aggregating indicators. In particular since a robust inter-comparison is possible with these indicators, which could not be derived from a limited

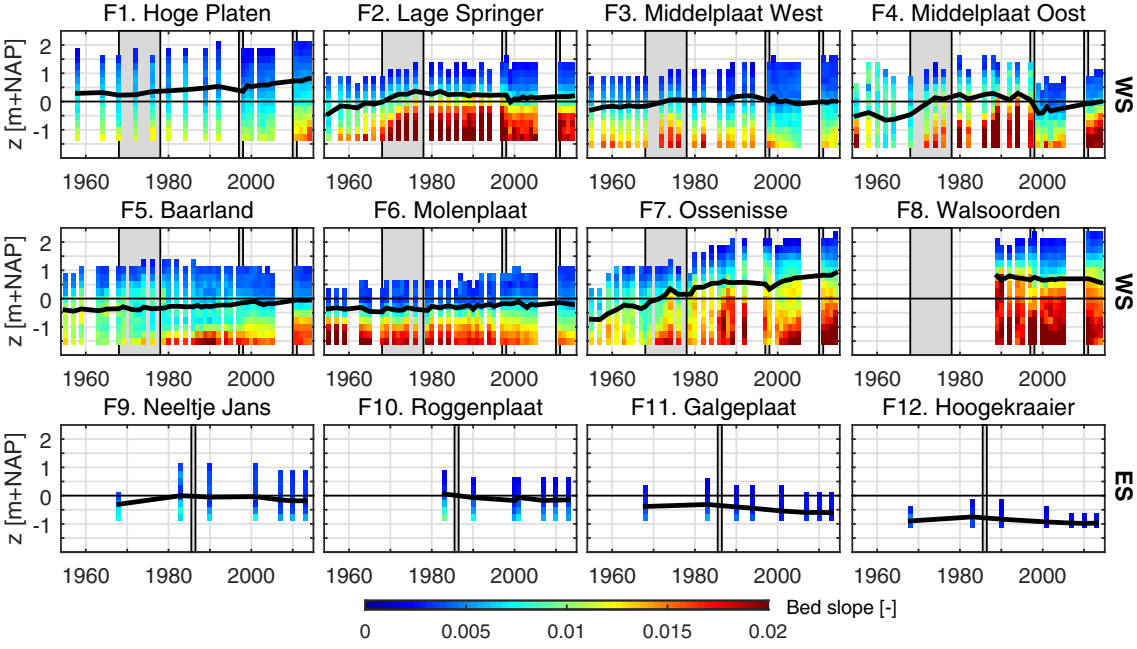


**Fig. 14.** Integral bed slope of the tidal flats over time, as calculated with the Vaklodingen dataset. The black line indicates the average height of the intertidal area. Bed slopes could be steeper than 0.02 (e.g., Fig. 10), but are limited in this figure to this value to distinguish also some of the vertical variation of the relatively mild ES flats. The vertical gray boxes on the background indicate the deepening projects in the WS and the completion of the storm surge barrier of the ES.

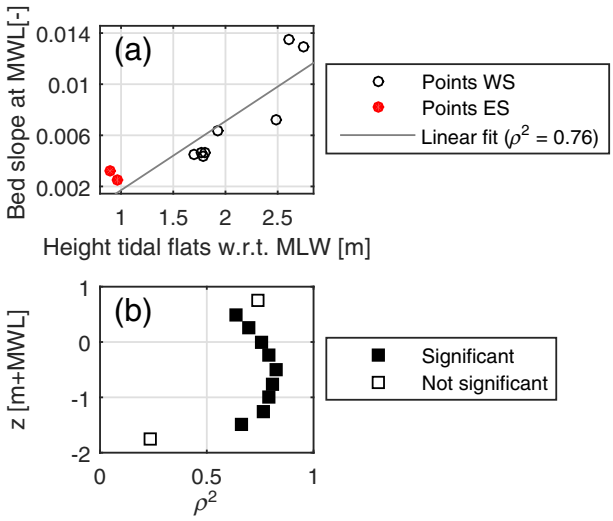


**Fig. 15.** The relation between the integral bed slope and the height of the intertidal areas for the 2013 LiDAR data: (a) at MWL; (b) at various other reference levels. The amount of flats with a bed slope calculated at a certain reference level varies as the tidal range differs per flat. Only reference levels with at least 5 data points are taken into account. A relation is considered as significant if the null hypothesis of no correlation can be rejected with a probability of 99% or more (*t*-test).

amount of cross-sections at arbitrary locations. As the different indicators could show completely different tendencies (e.g., Fig. 11), they should be considered simultaneously to properly account for the morphological changes.

Defining a robust estimate for "the" height of an intertidal area is not trivial. Simply considering the highest bed level elevation of a flat is undesirable, as it is doubtful how representative that single value is for the full intertidal area. Furthermore, the measurement method and resolution could affect this value substantially. Instead, this study considered the average height of a tidal flat, by dividing the total sediment volume between MLW and MHW by the area of the intertidal region, as expressed with Eq. (1). However, an intertidal area does not necessarily shift uniformly in the vertical plane (Figs. 9 and 13). By pure erosion around MLW, the area of the low region of a flat will reduce, causing the average height to increase (e.g., Middelplaat West (F3) in Fig. 9). Based on these considerations, the average height of the intertidal flat should be considered as an indicator for the vertical distribution of the sediment volume, not as a direct representation of the top of the flat.

The tidal range is kept constant over time in the analyses, to allow a direct comparison of the morphology between the different years. This has no implications for the evolution of the bed slope over time, as these are calculated with respect to a fixed reference frame (NAP). However, the area and volume estimates depend directly on the considered tidal range. As the tidal range in the WS was smaller in the past (Van den Berg et al., 1996), the area and volume of the intertidal flats are slightly overestimated for these past years. These quantities are underestimated in the ES for the years before the completion of the storm surge barrier, as this barrier reduced the tidal range substantially.

### 5.2. Relation between height and steepness of intertidal areas

The relation between the height of the intertidal areas and their steepness, as suggested by Fig. 15, should not be considered as a universal law. For instance, a flattening of the lower zone of Molenplaat (F6) did not coincide with an average lowering of this flat. Still, this relation appeared to be a good indicator for many flats. Fig. 17a illustrates this relation to satisfy the geometrical extremes: a flat with an extremely high average intertidal height (almost MHW) will be almost infinitely steep as hardly any bed level elevations are between MLW and MHW, whereas an extremely low intertidal flat (i.e., average height just above MLW) would be extremely mild. Furthermore, a homogeneous lowering of an idealised convex-up (e.g., parabolic) tidal flat, with its top below the MHW level, would induce a flattening of the bed at all elevations (see Fig. 17b). Such a vertical translation in the bed slope profile is not that unrealistic for real world flats (e.g., Fig. 14). At certain elevations, the bed slope might flatten less (or even steepen), if the shape of the flat changes. Nevertheless, the bed slope has to decrease at least at some elevations to satisfy the geometrical constraint of a horizontal top of the intertidal area. Therefore, the lowering of a flat should coincide with at least some flattening of an intertidal area, and the heightening with at least some steepening.

With the presence of channels nearby intertidal areas, a horizontal expansion of an accretive tidal flat could be counteracted by the transport capacity of those channels. For an intertidal area which is located closely to a channel, such as Ossenisse (F7), the flat could only increase in volume by a steepening, a migration of the side of the channel or a combination of both. If such a migration is not possible, only a steepening allows those horizontally constraint tidal flats to increase in volume (i.e., heighten).

### 5.3. Differences in morphological development between the ES and WS

The differences in morphological evolution between the intertidal flats of both systems are probably related to the differences in hydrodynamic forcing. This hypothesis is strengthened by the fact that the intertidal areas in the ES were in a dynamic equilibrium or even slightly heightening before the construction of the storm surge barrier (Louters et al., 1998; Mulder and Louters, 1994). After the construction of this barrier, the intertidal areas of the ES have been eroding strongly (Fig. 11). This change in trend is most likely related to changes in hydrodynamics imposed by the barrier.

Fig. 4b presents a spatial overview of the depth-averaged flow velocities in both estuaries. The flow velocities in the main channels of the WS are significantly larger than those in the ES. There are various reasons for the differences in flow velocities. First, the flow velocities in the ES are reduced by the presence of the storm surge barrier and compartment dams (Louters et al., 1998; Eelkema et al., 2009). The tide propagates far upstream in the River Scheldt, whereas the tidal propagation in the ES is limited by the closure of its branches (i.e., limited tidal prism). Second, the substantially larger tidal range in the WS (see Fig. 4a) implies a relatively larger ebb/flood volume.

Comparing the wave forcing between both estuaries is challenging, as the wave characteristics depend highly on the considered wave climate. We expect the waves in both systems to be mainly generated locally, as the geometry of the WS and the presence of the storm surge barrier in the ES do not allow sea waves to propagate deeply into the estuaries. Within the estuaries, there is a variability of the wave energy by a natural inhomogeneity in local fetch. This inhomogeneity causes also a variation in the wave climate at different sides of a tidal flat, which could therefore evolve differently (e.g., Fig. 16). However, both estuaries contain flats with a relatively large fetch and flats with a relatively short fetch, as the ES and WS have a similar geometry. Furthermore, the wind climate in both estuaries is comparable (see Fig. 3). Therefore, the wave forcing on itself is not considered as the explanatory variable for the differences observed in the evolution of the flats between the two estuaries.

Based on these considerations, the tidal flow with respect to the wave forcing is relatively large in the WS and relatively small in the ES. A relatively large tidal forcing is in line with increased deposition on the tidal flats, whereas increased wave forcing coincides with increased erosion (Friedrichs, 2011; Green and Coco, 2014).

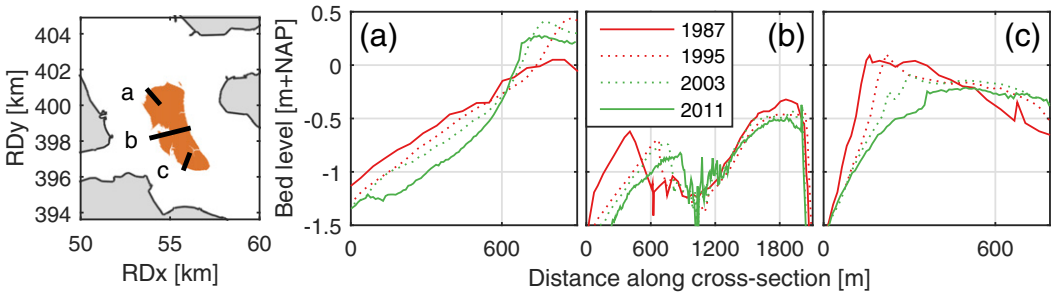


**Fig. 16.** RTK-dGPS cross-section data at Galgeplaat (F11) shown over a uniform eight year interval. The distances along the cross-sections are with respect to the most western point of each cross-section.

Therefore, this theoretical insight supports the suggestion that the differences in morphological response between both estuaries are closely related to the differences in flow velocities.

For a more detailed understanding of the changes of the intertidal flats in both estuaries, more research on the local characteristics of individual flats is required. Besides the considered processes, also the net import/export of sediment for an estuary (De Vriend et al., 2011; Yang et al., 2006), the seasonal variability of mud content (Pethick, 1996) and the differences in sediment characteristics play a role in these changes. These have not been included in this study as a robust inter-comparison between individual flats becomes less trivial.

### 5.4. Future fate of the intertidal areas

The data analysed in this paper provided various insights on the historical evolution of the considered intertidal areas. Although the future changes of the tidal flats are not necessarily a simple extrapolation of the historical evolution, valuable considerations can be drawn by combining the insights from the historical evolution with expected future conditions (e.g., sea level rise).

With ongoing human interference, both systems are expected to evolve towards a new equilibrium (De Vriend et al., 2011; Wang et al., 2015). This is thought to be a dynamic equilibrium as changes in the hydrodynamic forcing are ongoing. In this study, the tidal datums are considered to be constant over time. However, in reality these tidal datums are affected by sea level rise (Mawdsley et al., 2015) and dredging activities (Kuijper and Lescinski, 2013). Mawdsley et al. (2015) indicate that the MLW and MHW datums do not change necessarily with the same rate and direction as the mean sea level. With the uncertainty of future sea level rise rates and the complexity of the spatial inhomogeneity of the changes of the tidal datums, the temporal changes of the datums are not considered in this study.

No simple linear relations could describe the evolution of the intertidal flats in the WS on the time scale of half a century (see Fig. 11). Still, the flats in the WS increased in height on average almost 1 cm per year over this period, which is substantially larger than the faced sea level rise rate. As the fairly high Hoge Platen (F1) has still been rising substantially over past years (see Fig. 9), there is no indication that the heightening of the flats in the WS will be limited in the near future. In fact, marsh vegetation could establish on the high intertidal elevations (Kirby, 2000), which will increase the resistance against erosion (Eerdt, 1985). Hoge Platen (F1) is an example of a flat in the WS on which vegetation is expanding rapidly over recent years. If the heightening coincides with a steepening of the flats, the natural habitats are expected to impoverish even further (De Jong and De Jonge, 1995).

Although the long-term data in the ES is scarce, there is strong evidence for a consistent lowering of the flats (in line with Louters et al., 1998). Fig. 11 indicates that the erosion of the intertidal areas started directly after the completion of the storm surge barrier, with an average rate of approximately 0.7 cm per year. An important difference with the continuous dredging activities in the WS is the almost instantaneous introduction of the human interventions to the ES. Consequently, the lowering rate of the flats in the ES might eventually decrease when the intertidal areas approach an equilibrium height (also argued by Louters et al., 1998). The most recent data indicates a slight change in trend of the average height evolution after 2007 in both the Vaklodingen data as in many of the more frequently measured cross-sections. However, future measurements should reveal whether a long-term equilibrium of the bulk quantities is approached, and if those flats are able to cope with sea level rise.

## 6. Summary and conclusions

This paper has analysed the present state and long-term development of the intertidal areas in the ES and WS based on robustly defined bulk parameters. The flats in the WS are identified as substantially higher and steeper compared to those in the ES. None of the studied intertidal flats is found to be in a static equilibrium. The differences in the morphology of the flats between both estuaries increased over the past decades, by rising flats in the WS and lowering flats in the ES. Over the past 59 years, the flats in the WS did not change monotonously: the area, volume and average height of those flats fluctuated substantially. Still, the average height of the WS flats increased with 1 cm per year on average over this period. In the ES, a change in trend is observed. The considered flats lowered with an average rate of 0.7 cm per year after the completion of the storm surge barrier, despite the recently reduced erosion rates.

A larger steepness of intertidal flats has been related to a larger average height. This relation appeared not only from the present state of the intertidal flats, but was also observed in the change of the

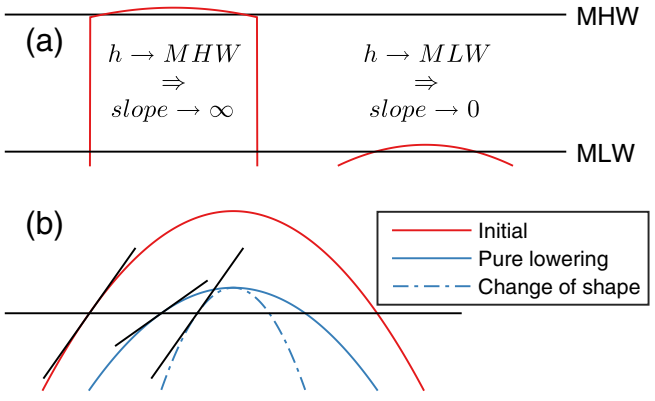


**Fig. 17.** Cross-sections of idealised tidal flats to illustrate: (a) the relation of the extremes of the average height of a flat with the extremes of the bed slopes and (b) the reduced bed slope caused by the lowering of tidal flats.

bed slopes of individual flats over time. Although there is evidence for steepening flats in the WS and flattening flats in the ES, not all flats changed with this tendency, and the changes in steepness were not necessarily uniform over depth.

The differences in tidal flow velocities between the ES and WS, for a substantial part caused by human interventions, are thought to explain an important part of the opposed morphological developments of the intertidal areas between both estuaries. It is expected that the observed morphological changes in the WS will continue. However, the recently reduced erosion rates of the flats in the ES could indicate the approach of an equilibrium.

## Acknowledgements

This work was supported by the Netherlands Organisation for Scientific Research (NWO) via the project "EMERGO - Eco-morphological functioning and management of tidal flats" (850.13.021). All the data presented in this paper are surveyed by Rijkswaterstaat. Special thanks to Edwin Paree, Jan de Bel and Marco Schrijver from Rijkswaterstaat for providing these datasets. We gratefully acknowledge two anonymous reviewers for their constructive comments.

## References

Bearman, J.A., Friedrichs, C.T., Jaffe, B.E., Foxgrover, A.C., 2010. Spatial trends in tidal flat shape and associated environmental parameters in South San Francisco Bay. J. Coast. Res. 262, 342–349. http://dx.doi.org/10.2112/08-1094.1.

Bolle, A., Wang, Z.B., Amos, C., De Ronde, J., 2010. The influence of changes in tidal asymmetry on residual sediment transport in the Western Scheldt. Cont. Shelf Res. 30, 871–882. http://dx.doi.org/10.1016/j.csr.2010.03.001.

Boon, J.D., Byrne, R.J., 1981. On basin hyposmetry and the morphodynamic response of coastal inlet systems. Marine Geology 40, 27–48. http://dx.doi.org/10.1016/0025-3227(81)90041-4.

Cancino, L., Neves, R., 1999. Hydrodynamic and sediment suspension modelling in estuarine systems. J. Mar. Syst. 22, 117–131. http://dx.doi.org/10.1016/S0924-7963(99)00036-6.

Cleveringa, J., 2013. Ontwikkeling mesoschaal Westerschelde: factsheets. Technical Report International Marine & Dredging Consultants/Deltares/Svašek Hydraulics BV/ARCADIS Nederland BV Antwerp (in Dutch).

De Jong, D.J., De Jonge, V.N., 1995. Dynamics and distribution of microphytobenthic chlorophyll-a in the Western Scheldt estuary (SW Netherlands). Hydrobiologia 311, 21–30. http://dx.doi.org/10.1007/BF00008568.

De Vriend, H.J., Wang, Z.B., Ysebaert, T., Herman, P.M.J., Ding, P., 2011. Eco-morphological problems in the Yangtze Estuary and the Western Scheldt. Wetlands 31, 1033–1042. http://dx.doi.org/10.1007/s13157-011-0239-7.

Dieckmann, R., Osterthun, M., Partenscky, H.-W., 1987. Influence of water-level elevation and tidal range on the sedimentation in a German tidal flat area. Prog. Oceanogr. 18, 151–166. http://dx.doi.org/10.1016/0079-6611(87)90031-0.

Dyer, K., Christie, M., Wright, E., 2000. The classification of intertidal mudflats. Cont. Shelf Res. 20, 1039–1060. http://dx.doi.org/10.1016/S0278-4343(00)00011-X.

Eelkema, M., Wang, Z., Stive, M., 2009. Historical morphological development of the Eastern Scheldt tidal basin (The Netherlands). Coastal Dynamics 2009, 6th International Conference, Tokyo, Japan, September 7–11 2009, Paper No. 85. World Scientific Publishing., http://dx.doi.org/10.1142/9789814282475_0087.

Eerdt, M.M., 1985. The influence of vegetation on erosion and accretion in salt marshes of the Oosterschelde, The Netherlands. Vegetatio 62, 367–373. http://dx.doi.org/10.1007/BF00044763.

Eisma, D., 1998. Intertidal Deposits: River Mouths, Tidal Flats, and Coastal Lagoons. CRC Press, Boca Raton.

Friedrichs, C.T., 2011. Tidal flat morphodynamics: a synthesis. In: Wolanski, E., McLuskyDonald (Eds.), Treatise on Estuarine and Coastal Science Chapter 3.06. Elsevier, Waltham, pp. 137–170. http://dx.doi.org/10.1016/B978-0-12-374711-2.00307-7.

Fujii, T., Raffaelli, D., 2008. Sea-level rise, expected environmental changes, and responses of intertidal benthic macrofauna in the Humber estuary, UK. Mar. Ecol.: Prog. Ser. 371, 23–35. http://dx.doi.org/10.3354/meps07652.

Green, M.O., Coco, G., 2014. Review of wave-driven sediment resuspension and transport in estuaries. Rev. Geophys. 52, 77–117. http://dx.doi.org/10.1002/2013RG000437.

Kirby, R., 2000. Practical implications of tidal flat shape. Cont. Shelf Res. 20, 1061–1077. http://dx.doi.org/10.1016/S0278-4343(00)00012-1.

Kohsiek, L., Mulder, J., Louters, T., Berben, F., 1987. De Oosterschelde naar een nieuw onderwaterlandschap. Technical Report Rijkswaterstaat, RIKZ Goes (in Dutch).

Kuijper, K., Lescinski, J., 2013. Data-analysis water levels, bathymetry Western Scheldt. Technical Report International Marine & Dredging Consultants/Deltares/Svašek Hydraulics BV/ARCADIS Nederland BV Antwerp.

Le Hir, P., Roberts, W., Cazaillet, O., Christie, M., Bassoullet, P., Bacher, C., 2000. Characterization of intertidal flat hydrodynamics. Cont. Shelf Res. 20, 1433–1459. http://dx.doi.org/10.1016/S0278-4343(00)00031-5.

Lesser, G., Roelvink, J., van Kester, J., Stelling, G., 2004. Development and validation of a three-dimensional morphological model. Coast. Eng. 51, 883–915. http://dx.doi.org/10.1016/j.coastaleng.2004.07.014.

Louters, T., van den Berg, J.H., Mulder, J.P.M., 1998. Geomorphological changes of the Oosterschelde tidal system during and after the implementation of the delta project. J. Coast. Res. 14, 1134–1151.

Marijs, K., Paree, E., 2004. Nauwkeurigheid vaklodingen Westerschelde en -monding "de praktijk". Technical Report Meetinformatiedienst Zeeland Vlissingen (in Dutch).

Mawdsley, R.J., Haigh, I.D., Wells, N.C., 2015. Global secular changes in different tidal high water, low water and range levels. Earth's Futur. 3, 66–81. http://dx.doi.org/10.1002/2014EF000282.

Mulder, J.P.M., Louters, T., 1994. Changes in basin geomorphology after implementation of the Oosterschelde Estuary project. Hydrobiologia 282-283, 29–39. http://dx.doi.org/10.1007/BF00024619.

Murray, N.J., Clemens, R.S., Phinn, S.R., Possingham, H.P., Fuller, R.A., 2014. Tracking the rapid loss of tidal wetlands in the Yellow Sea. Front. Ecol. Environ. 12, 267–272.

Pethick, J.S., 1996. The geomorphology of mudflats. In: Nordstrom, K.F., Roman, C.T. (Eds.), Estuarine Shores: Evolution, Environments and Human Alterations Chapter 8. John Wiley & Sons, Chichester, pp. 185–211.

Pezij, M., 2015. Understanding and Modelling of the Oesterdam Nourishment. University of Twente. Msc thesis

Santinelli, G., de Ronde, J., 2012. Volume analysis on RTK profiles of the Eastern Scheldt. Technical Report. Deltares, Delft.

Smaal, A., Nienhuis, P., 1992. The eastern Scheldt (The Netherlands), from an estuary to a tidal bay: a review of responses at the ecosystem level. Neth. J. Sea Res. 30, 161–173. http://dx.doi.org/10.1016/0077-7579(92)90055-J.

Stanev, E.V., Flöser, G., Wolff, J.-O., 2003. First- and higher-order dynamical controls on water exchanges between tidal basins and the open ocean. A case study for the East Frisian Wadden Sea. Ocean Dyn. 53, 146–165. http://dx.doi.org/10.1007/s10236-003-0029-8.

Strahler, A.N., 1952. Hypsometric (area-altitude) analysis of erosional topography. Geological Society of America Bulletin 63, 1117–1142. http://dx.doi.org/10.1130/0016-7606(1952)63[1117:HAAOET]2.0.CO;2.

Van Eck, B., 1999. De Scheldeatlas: een beeld van een estuarium. Technical Report Rijksinstituut voor Kust en Zee/Schelde Middelburg (in Dutch).

Van den Berg, J.H., Jeuken, C.J.L., Van der Spek, A.J.F., 1996. Hydraulic processes affecting the morphology and evolution of the Westerschelde estuary. In: Nordstrom, K.F., Roman, C.T. (Eds.), Estuarine Shores: Evolution, Environment and Human Alterations Chapter 7. John Wiley & Sons, Chichester, pp. 157–184.

Van der Werf, J., Van Oyen, T., De Maerschalck, B., Nnafie, A., Van Rooijen, A., Taal, M., Verwaest, T., De Vet, L., Vroom, J., Van der Wegen, M., 2015. Modeling the morphodynamics of the mouth of the Scheldt estuary. E-proceedings of the 36th IAHR World Congress. The Hague., pp. 80–86.

Wang, Z.B., Jeuken, M.C.J.L., Gerritsen, H., de Vriend, H.J., Kornman, B.A., 2002. Morphology and asymmetry of the vertical tide in the Westerschelde estuary. Cont. Shelf Res. 22, 2599–2609. http://dx.doi.org/10.1016/S0278-4343(02)00134-6.

Wang, Z.B., Van Maren, D.S., Ding, P.X., Yang, S.L., Van Prooijen, B.C., De Vet, P.L.M., Winterwerp, J.C., De Vriend, H.J., Stive, M.J.F., He, Q., 2015. Human impacts on morphodynamic thresholds in estuarine systems. Cont. Shelf Res. CSR3681. http://dx.doi.org/10.1016/j.csr.2015.08.009.

Wiegmann, N., Perluka, R., Oude Elberink, S., Vogelzang, J., 2005. Vaklodingen: de inwintechnieken en hun combinaties: vergelijking tussen verschillende inwintechnieken en de combinaties ervan. Technical Report Adviesdienst Geo-Informatica en ICT (AGI) Delft (in Dutch).

Wilson, M.A., Costanza, R., Boumans, R., Liu, S., 2005. Integrated assessment and valuation of ecosystem goods and services provided by coastal systems. In: Wilson, J.G. (Ed.), The Intertidal Ecosystem: The Value of Ireland's Shores Chapter 1. Royal Irish Academy, Dublin, pp. 1–24.

Wolff, W., 1973. The Estuary as a Habitat: An Analysis of Data on the Soft-bottom Macrofauna of the Estuarine Area of the Rivers Rhine, Meuse, and Scheldt. Leiden University. Phd thesis

Yang, S.L., Li, M., Dai, S.B., Liu, Z., Zhang, J., Ding, P.X., 2006. Drastic decrease in sediment supply from the Yangtze River and its challenge to coastal wetland management. Geophysical Research Letters 33, L06408. http://dx.doi.org/10.1029/2005GL025507.